Studies of climatic change with zonally averaged models

by

V. Brahmananda Rao and Sergio H. Franchito

Instituto Nacional de Pesquisas Espaciais-INPE
CP 515, 12201, São José dos Campos, SP, Brazil

RESUMEN

En este artículo se incluye un breve repaso a la clasificación de modelos climáticos basados en grados de libertad, mencionando las ventajas de los que se aplican a promedios zonales (ZACM). Concretamente, los dos modelos que se describen, uno cuasi-geostrófico (QG) y otro más completo de ecuaciones primitivas (PE), se utilizan para realizar experimentos numéricos sobre el cambio climático inducido por anomalías en la temperatura de la superficie del mar (SST) y por alteraciones en las características de los suelos. Los experimentos relativos a anomalías en la SST consideran las situaciones correspondientes a los conocidos fenómenos de El Niño y La Niña. Los resultados muestran que durante El Niño, tanto la corriente en chorro subtropical como la circulación de Hadley se intensifican y la temperatura superficial del mar aumenta en la región perturbada. En el caso de La Niña se observa la situación opuesta. Por otra parte, en el experimento correspondiente a alteraciones en las características del suelo se consideran los efectos inducidos por procesos geobotánicos (deforestación y desertificación) en el clima. Los resultados muestran que la alteración en la temperatura del suelo se debe más al cambio en el ritmo de evapotranspiración que en el del albedo.

ABSTRACT

A brief review of the classification of climate models based on degrees of freedom is given. The advantages of zonally averaged climate models (ZACM) are mentioned. Two ZACM are described, a simple quasi-geostrophic (QG) model and a more complete pimitive equations (PE) global model. These are used to conduct numerical experiments regarding the climatic change due to sea surface temperatures (SST) anomalies and land surface alterations. The experiments regarding the SST anomalies consider the situations of El Niño and La Niña. The results show that in the El Niño situation the subtropical jet stream and the Hadley circulation are intensified and surface temperature increased in the perturbed region. The opposite situation occurs in the case of La Niña. In the experiment of surface state modification the interaction between the geobotanic state and the climate is considered. Experiments are conducted regarding deforestation and desertification. The results show that the change in the evapotranspiration rather than the change in the surface albedo is the predominant effect in regulating the changes in the surface temperature.

1. INTRODUCTION

The earth's climate changes. It has changed many times in the past, it is changing now and in the future it will continue to evolve. Climatic change could be partly natural and partly man made. Climatic change due to fluctuation in the earth's orbit is an example of natural cause. Future climatic change unlike that of the past can partly be affected by human activity. One human activity which has received much attention recently is the increase of pollution with gases such as carbon dioxide. Measurements unambiguously show that carbon dioxide has increased by about 25 % during the last century. Whether the recent increase in temperature at earth's surface (Jones *et al.*, 1986a; Jones *et al.*, 1986b; Karoly, 1987) is due the increase of carbon dioxide is still somewhat controvertial (Idso and Mitchell, 1989; Lindzen, 1990). Another human activity which again has important implication for climatic change is the land surface alteration such as deforestation (Dickinson and Henderson-Sellers, 1988; Dickinson, 1989; Shukla *et al.*, 1990).

Undoubtedly it would be necessary to know the future climatic change to get preared for such a change. Future climatic change can be inferred by means of mathematical models. Like any natural phenomenon, climate and its change are presumably governed by physical laws. These physical laws can be written in terms of mathematical expressions which constitute a model. Computer can be utilized to calculate how climate will evolve in time in accordance with the laws.

The complexity of climate models together with the limitations in computational resources necessitates simplifications and assumptions. This led to the development of a hierarchy of climate models. Climate models can be classified on the basis of the degrees of freedom (Schneider and Dickinson, 1974).

The simplest climate models are the one-dimensional radiative-convective models (RCM) (Manabe and Wetherald, 1967; Rasool and Schneider, 1971). The RCM usually incorporate relatively detailed treatment of radiative processes and permit for example investigation of the consequences of global scale changes in atmospheric composition. Normally RCM give only the vertical profile of global mean temperature.

Within the class of one-dimension climate models lie the energy balance models (EBM) wherein vertical integration is done in order to treat latitudinal variation of the climate in terms of surface temperature (Budyko, 1969; Sellers, 1969).

More complex climate models are the general circulation models (GCM) which are used in the studies aimed at obtaining detailed evolution of regional and seasonal behaviour of climate. In these models the behaviour of climate is determined explicity. The explicit calculations of the complete synoptic atmospheric (oceanic) behaviour can make the system being modelled as complex as the real system which makes it difficult to analyse and understand. Furthermore GCM require large computing facilities.

An intermediate class of models are the zonally averaged climate models (ZACM) in which the treatment of radiative proceses can be as sophisticated as in the GCM but somewhat simplified from the detailed RCM. While the RCM and EBM consider only the thermodynamics of the system, ZACM includes the treatment of dynamics usually by allowing two atmospheric layers. Although the synoptic systems are not included explicitly, their statistical effects are included through parameterization (Saltzman and Vernekar, 1968; Saltzman and Vernekar, 1971; Saltzman and Vernekar, 1972; Stone, 1974; Stone and Yao, 1987). Because of this, ZACM are sometimes referred to as statistical dynamical climate models, although some (eg. Saltzman, 1978) prefer to a make a further distintion. Another advantage of ZACM in comparison with RCM and EBM is the inclusion of both latitudinal and vertical variation, thereby permitting more explicit treatment of many feedback mechanisms. Some of the recent ZACM even include oceanic coupling also (Harvey, 1988a; Harvey, 1988b). Because of their simplicity compared to GCM, they require far less computer time. Of course some of the advantages are counterbalanced by loss of regional resolution and also the errors and limitations are necessarily introduced in the process of parameterization.

Because of their intermediate position, ZACM can be helpful in the design and analysis of GCM studies and in generalizing the results of simple EBM and RCM studies. Thus ZACM can be thought of as making a bridge between simpler EBM and sophisticated GCM.

The most important simplification made in ZACM compared to GCM is the parameterization of eddy fluxes of heat and momentum. Meridional transport of heat is parameterized using exchange coefficient (Adem, 1962; Saltzman, 1968; Green, 1970 and others). The parameterization of eddy momentum flux is much more difficult because it is up the gradient of angular velocity and because of this a simple treatment of diffusion is not possible, unless one contends to use negative exchange coefficients. Saltzman and Vernekar (1968) developed a sophisticasted parameterization of momentum transport. Wiin-Nielsen and Sela (1971) have shown using observed data that it is possible to parameterize the momentum transport indirectly through the use of exchange coefficient for quasi-geostrophic potential vorticity and for heat. Sela and Wiin-Nielsen (1971), Ohring and Adler (1978) and Gutman *et al.* (1984) have shown that such a parameterization can be used successfully in ZACM.

Tests of sensitivity due to changes in the boundary conditions can be investigated using ZACM. Ohring and Adler (1978) studied the effect of changes in the amount of carbon dioxide, in the solar constant and in the cloud content. Potter and Cess (1984) and Jung and Bach (1987) investigated the effect of aerosols on the distribution of zonally averaged temperature. Another example of the study of sensitivity is the impact of sea surface temperature (SST) anomalies on atmospheric circulation. The effect of SST anomalies is studied using GCM (Shukla and Wallace, 1983; Lau and Oort, 1985; Moura and Shukla, 1981). Nevertheless, ZACM can be used to determine the range of variations due the impact of SST anomalies. One such example is the study of Wiin-Nielsen (1986) regarding the El Niño situation.

Recently much effort has been dedicated in the study of interaction between surface characteristics (vegetation, soil moisture, etc) and the overlying atmosphere. A model which includes these biogeophysical feedback (biofeedback) mechanisms can be used to test hypotheses regarding the climate modification due to changes in the surface characteristics which can be natural or man made. Complex parameterizations of biosphere have been incorporated in sophisticated climate models (Mintz *et al.*, 1983; Sellers *et al.*, 1986; Dickinson *et al.*, 1986; Dickinson and Henderson Sellers, 1988; Shukla *et al.*, 1990)

. However, considering that these GCM involve many complex processes it is difficult to trace the exact cause of a given effect. So simple ZACM are useful in this context. Also ZACM are more economical for conducting a large number of experiments concerning long term climatic changes.

In spite of the usefulness of ZACM only a few studies have been made with these models regarding the climatic effects caused by surface alterations. One of the pionering studies in this line was that of Charney *et al.* (1975). Using a quasi-geostrophic model without the consideration of hydrological cycle, they showed that increase of albedo produced subsidence which perpetuated desert conditions.Ellsaesser *et al.* (1976) and Potter *et al.* (1975) conducted experiments of desertification and deforestation respectively. Gutman *et al.* (1984) using a version of the Ohring and Adler (1978) hemispheric quasi-geostrophic ZACM incorporated a parameterization of biofeeback mechanism. Gutman (1984) studied the hemispheric response of land surface alteration like deforestation, desertification and irrigation. However Gutman *et al.* (1984) considered only the Northern Hemisphere (NH).

In the present article we describe two ZACM: 1) a quasi-geostrophic model similar to that of Sela and Wiin-Nielsen (1971) extended to the Southern Hemisphere (SH). New exchange coefficients using the observed data are also determined. 2) a primitive equations model similar to that of Taylor (1980). Taylor's model neglected latent heating and evaporative cooling. Another physical process not included in Taylor's model is the subsurface conduction in the surface heat balance. All these physical processes in the present model in addition to biofeedback mechanism are similar to those of Gutman *et al.* (1984). In section 2 the quasi-geostrophic model together with the experiments of El Niño and La Niña are given. In section 3 the primitive equations model is described together with the experiments of deforestation and desertification. In section 4 the summary is given.

2. STUDIES WITH A ZONALLY AVERAGED QUASI-GEOSTROPHIC CLIMATE MODEL

In this section a brief description of a zonally averaged quasi-geostrophic model is given. In addition the calculations of the transport of quasi-geostrophic potential vorticity and the exchange coefficients for the NH and SH which are necessary for the formulations of the model are given. Numerical experiments conducted with the model regarding the climate effects due to the anomalies of SST, particulary the cases of El Niño and La Niña are also presented.

a) Quasi-geostrophic potential vorticity transport and the determination of the exchange coefficients.

The procedure for the calculation of the meridional transport of quasi-geostrophic potential vorticity ($\overline{Qv}$) has been described in detail by Wiin-Nielsen and Sela (1971). So here we only present briefly the method giving the necessary formulae. The meridional transport of quasi-geostrophic potential vorticity may be evaluated using the formula:

$$\overline{Qv} = -\frac{1}{\mathrm{a}\cos^2\phi}\frac{\partial}{\partial\phi}(\overline{uv})\cos^2\phi - \frac{\partial}{\partial p}\left[\frac{f_0 R}{\overline{\sigma} p}(\overline{Tv})\right] \qquad [1]$$

where $\overline{uv}$ is the meridional eddy momentum transport; $\overline{Tv}$, the eddy heat transport; R, the gas constant; ϕ, the latitude; p, the pressure; a, The earth's radius; $\overline{\sigma}$, the static stability parameter, and f_0 the Coriolis parameter at a reference latitude, say, 45° N(S).

From equation (1) the meridional transport of quasi-geostrophic potential vorticity can be computed using the data of the momentum transport and the heat transport. Franchito and Rao (1991) evaluated $\overline{Qv}$ for both the hemispheres using the data of Oort and Rasmusson (1971) for the NH and the data from the National Meteorological Center (NMC) for the SH.

Figures 1 and 2 show the computed values of $\overline{Qv}$ for the NH and SH, respectively. It can be seen that the transport of quasi-geostrophic potential

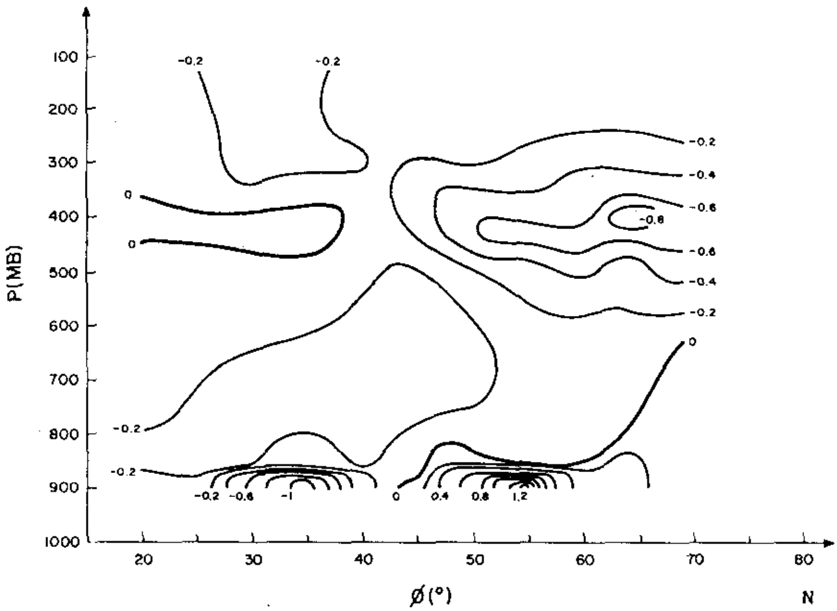

Figure 1.—Annual mean meridional transport of quasi-geostrophic potential vorticity as funtion of latitude and pressure for the NH calculated from the data of Oort and Rasmusson (1971) (units 10^{-4} m s^{-2}).

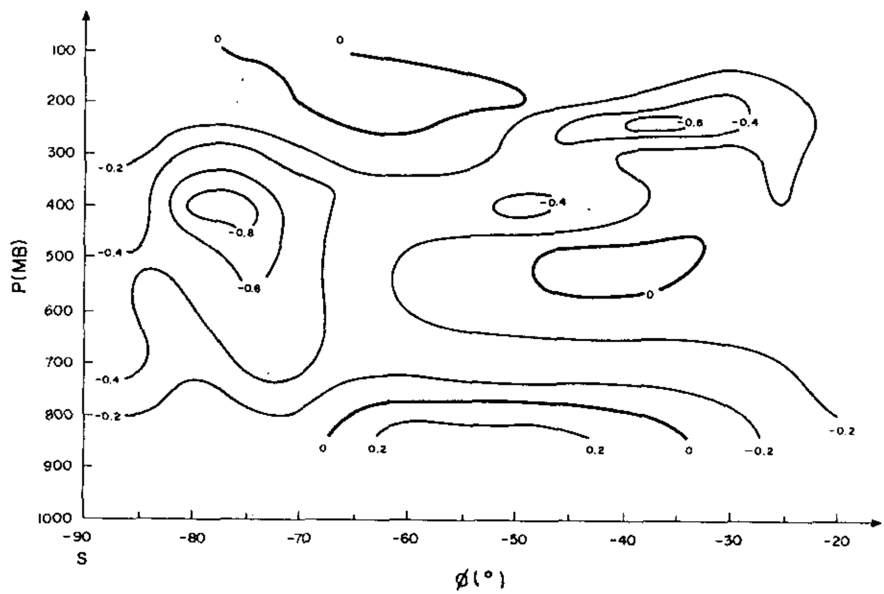

Figure 2.—Annual mean meridional transport of quasi-geostrophic potential vorticity as a function of latitude and pressure for the SH calculated from the NMC data (units 10^{-4} m s^{-2}).

vorticity is qualitatively similar in both the hemispheres. The transport is negative over most of the atmosphere except over a thin layer near the surface where it is positive. The characteristic of $\overline{Qv}$ shown in these figures have interesting implications for dynamics of baroclinic waves. The change of direction of $\overline{Qv}$ due to a thin region of positive transport near the surface satisfies the requirement for baroclinic instability to occur in the troposphere (Charney and Stern, 1962; Scheneider and Dickinson, 1974). Furthermore, the regions of negative $\overline{Qv}$ in the free atmosphere are the regions of convergence of Eliassen and Palm flux (Edmon *et al.*, 1980) and the thin region of positive $\overline{Qv}$ near the surface is equivalent to this divergence. This agrees well with the characteristics of baroclinic waves discussed by Edmon *et al.* (1980) and Randel and Stanford (1985).

The transport of potential vorticity can be parameterized in terms of an exchange coefficient and gradient of mean potential vorticity (Green, 1970; Wiin-Nielsen and Sela, 1971):

$$\overline{Qv} = - K_Q \frac{\partial \overline{Q}}{a \partial \phi} \qquad [2]$$

and

$$\frac{\partial \overline{Q}}{a \partial \phi} = \frac{2\Omega \cos\phi}{a} - \frac{1}{a^2} \frac{\partial}{\partial \phi} \left[\frac{1}{\cos\phi} \frac{\partial \overline{u} \cos\phi}{\partial \phi} \right] - \frac{\partial}{\partial p} \left(\frac{f_0^2}{\overline{\sigma}} \frac{\partial \overline{u}}{\partial p} \right) \qquad [3]$$

where $\overline{Q}$ is the zonally averaged quasi-geostrophic potential vorticity; Ω, the earth's angular velocity, and $\overline{u}$, the zonal wind.

Using the values of $\overline{Qv}$ given in figures 1 and 2 the data of $\overline{u}$ given by Oort and Rasmusson (1971) for the NH and the NMC data for the SH, Franchito and Rao (1991) determined the values of K_Q for both the hemispheres, which are shown in figure 3 and figure 4. These values are used in the simple climate model described in the following.

b) Description of the model

The climate mobel is similar to that developed by Sela and Wiin-Nielsen (1971), which considers the zonally averaged form of the quasi-geostrophic potential vorticity equation. However, the parameterizations proposed by Saltzman (1986) rather than the Newtonian form of approximation are used for the diabatic heating. So, physical processes like shortwave solar radiation, longwave radiation, small-scale convection, evaporation and condensation, latent heat release, and subsurface conduction are incorporated in the model.

The prognostic equations are:

$$\frac{\partial \overline{Q}1}{\partial t} = \frac{1}{a^2 \cos\phi} \frac{\partial}{\partial \phi} \left(K_{Q1} \cos\phi \frac{\partial \overline{Q}1}{\partial \phi} \right) - \frac{q^2 R}{2 f_0 c_p} \overline{H}_a - 2A\overline{\zeta}_r \qquad [4]$$

$$\frac{\partial \overline{Q3}}{\partial t} = \frac{1}{a^2 \cos\phi} \frac{\partial}{\partial \phi}\left(K_{Q3} \cos\phi \frac{\partial \overline{Q3}}{\partial \phi}\right) + \frac{q^2 R}{2 f_0 c_p} \overline{H}_a + 2A\bar{\zeta}_T - \varepsilon\bar{\zeta}_* + 2\varepsilon\bar{\zeta}_T \quad [5]$$

where the overbar represents the zonal average and $\overline{Q}_1$ and $\overline{Q}_3$ are the quasi-geostrophic potential vorticity at 250 and 750 mb, respectively; $\overline{H}_a$, the atmospheric diabatic heating; K_{Q1} and $\overline{K_{Q3}}$, the exchange coefficients of $\overline{Q}_1$ and $\overline{Q}_3$, respectively; q^2, A and ϵ, are constants, given by Wii-Nielsen (1972), and $\bar{\zeta}_T$ and $\bar{\zeta}_*$ are given by

$$\bar{\zeta}_T = (\overline{Q}_1 - \overline{Q}_3)/2 + q^2 \overline{\psi}_T \quad [6]$$

$$\bar{\zeta}_* = (\overline{Q}_1 + \overline{Q}_3)/2 - f \quad [7]$$

The equation for the zonally averaged stream function $\overline{\psi}_T$ is

$$\frac{1}{a^2 \cos\phi} \frac{\partial}{\partial \phi}\left(\cos\phi \frac{\partial}{\partial \phi} \overline{\psi}_T\right) - q^2 \overline{\psi}_T = \frac{\overline{Q}_1 - \overline{Q}_3}{2} \quad [8]$$

The zonally averaged temperature at 500 mb ($\overline{T}_2$) is obtained using the relation:

$$\overline{\psi}_T = \frac{RT_2}{2f_0} \quad [9]$$

The zonally averaged surface temperature is obtained at each time step through the surface heat balance:

$$\sum_{1}^{M} \overline{H}_s\,(\mathrm{i}) = 0 \quad [10]$$

where $\overline{H}_s$ is the surface diabatic heating and M is the number of physical processes considered at surface.

The grid interval is 10° latitude. The initial state is an isothermal atmosphere (270 K) at rest. The equations are integrated using an implicit temporal scheme. The method of the tridiagonal matrix of Richtmeyer (1957) is used in the integration of equations (4), (5) and (8). The boundary conditions are:

$$\frac{\partial}{\partial \phi}(\overline{Q}_1, \overline{Q}_3, \overline{\psi}_T) = 0, \quad \phi = 0^0, 90^0 \text{ N (S)} \quad [11]$$

The zonally averaged vertical velocity $\overline{\omega}$ is calculated using the thermodynamic equation applied at 500 mb:

$$\omega = \frac{q^2 P_2}{f_0}\left[\frac{\partial}{\partial t}\overline{\psi}_T - \frac{1}{a^2 \cos\phi}\frac{\partial}{\partial \phi}\left(K_H \cos\phi \frac{\partial \overline{\psi}_T}{\partial \phi}\right) - \frac{R}{2 f_0 c_p}\overline{H}_a\right] \quad [12]$$

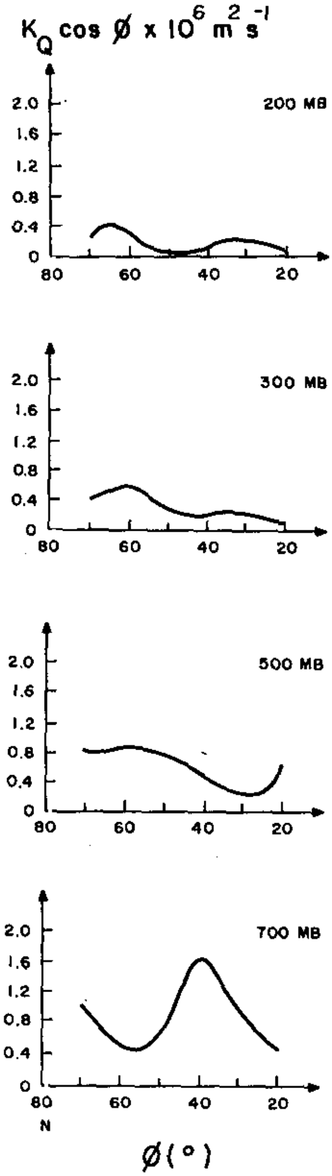

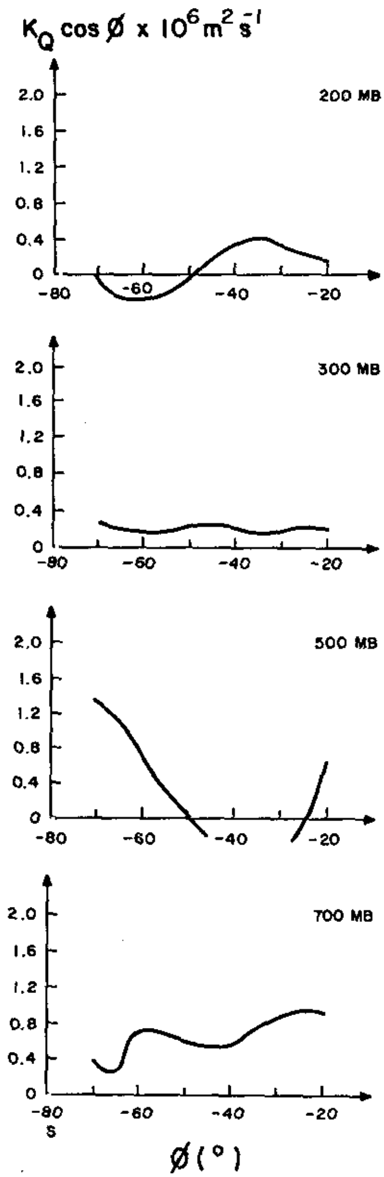

Figure 3.—Exchange coefficients for the transport of quasi-geostrophic potential vorticity as function of latitude for the levels 200, 300, 500 and 700 mb, calculated from mean annual data of Oort and Rasmusson (1971) for the NH (units $10^{-6}\ m^2\ s^{-1}$).

Figure 4.—Exchange coefficients for the transport of quasi-geostrophic potential vorticity as function of latitude for the levels 200, 300, 500 and 700 mb for the SH calculated from the NMC data (units $10^{-6}\ m^2\ s^{-1}$).

where $p_2 = 500$ mb and K_H is the exchange coefficient for the heat transport. K_H is calculated for both the NH and SH following the procedure given in Wiin-Nielsen and Sela (1971). The data used for this purpose are the same as mentioned earlier.

The functional forms of the diabatic heating are given in Table 1, where R_0 is the intensity of solar radiation at the top of atmosphere; r_a, the albedo of atmosphere; r_s, the surface albedo; χ, the opacity of the atmosphere to solar radiation; v_1 and v_2 the factors for downward and upward effective blackbody longwave radiation, respectively; σ_B the Stefan-Boltzman constant; $\overline{w}$, the water availability parameter; k, the factor proportional to the conductive capacity of surface medium; γ the longwave absorpivity of atmosphere; $\overline{T}_D$, the subsurface temperature; and b, c, e, and F are empirical constants given by Saltzman (1968).

Table 1. Functional forms for the diabatic heating.

i	$\overline{H}_s$ (i)	parameterization
1	shortwave solar radiation	$(1-\chi)(1-r_s)(1-r_a)\,R_0$
2	longware radiation	$\sigma_B(v_1\,\overline{T}_2^{\,4}-\overline{T}_s^{\,4})$
3	small scale convection	$-b((\overline{T}_s-\overline{T}_2)+c)$
4	evaporation and condensation	$\overline{w}(e\overline{H}_s(3)+F)$
5	subsurface conduction	$-k(\overline{T}_s-\overline{T}_D)$
i	$\overline{H}_a(i)$	parameterization
1	shortwave solar radiation	$\chi(1-r_a)\,R_0$
2	longwave radiation	$\sigma_B(v\overline{T}_s^{\,4}-(v_1+v_2)\,\overline{T}_2^{\,4})$
3	small-scale convection	$-\overline{H}_s(3)$
4	release of latent heat	$-\overline{H}_s(4)-La_4\,\overline{\omega}$

The formulation of $\overline{H}_a(4)$ in Table 1 is similar to that given by Gutman *et al.* (1984). This parameterization suggests that the precipitation is dependent on the evaporation and $\overline{\omega}$. L is the latent heat of vaporization and a_4 is an empirical constant.

In addition, the values of the water availability parameter ($\overline{w}$), the surface albedo (r_s) and subsurface temperature ($\overline{T}_D$) are obtained following the procedure given by Saltzman and Vernekar (1971, 1972):

$$\overline{w} = j_1\, w_{\text{ocean}} + j_2\, w_{\text{sea ice}} + j_3\, w_{\text{land}} + (j_4 + j_5)\, w_{\text{land ice}} \qquad [13]$$

$$r_s = j_1 r_{s\ \text{ocean}} + (j_2 + j_4 + j_5)\, r_{s\ \text{ice}} + j_3\, r_{s\ \text{land}} \qquad [14]$$

$$\overline{T}_D = j_1\, T_{DH} + (j_2 + j_3 + j_4 + j_5)\, T_{DL} \qquad [15]$$

where j_1, j_2 and j_3 are the fraction of ocean, sea ice and land; j_4 is the fraction of land covered by transient snow; j_5 is the fraction of land covered by permanent ice and snow; $\overline{T}_{DH}$ and $\overline{T}_{DL}$ are the subsurfaces temperatures in ocean and lithosphere, respectively.

c) Numerical experiments

The experiments presented here consider the case of anomalies of SST, in particular the situations of El Niño and La Niña. In these experiments the model is applied separately to both the hemispheres. The values and the localizations of the anomalies of SST are given in Table 2.

Table 2. Values and localizations of the anomalies of SST in the experiments of El Niño and La Niña.

El Niño		La Niña	
	$\Delta T\,(K)$		$\Delta T\,(K)$
15° N	0.5	15° N	1.0
5° N	2.0	5° N	−4.0
5° S	4.0	5° S	−4.0
15° S	2.0	15° S	1.0
25° S	−1.5		

The principal results (perturbed minus control) regarding the zonally averaged quantities: surface and 500 mb temperatures, zonal wind at 250 mb, vertical velocity at 500 mb, evaporation and precipitation are shown in figures 5-10, respectively. The experiment of El Niño is represented by full lines and the experiments of La Niña by dashed lines.

As can be seen in figures 5-10 the most notable deviations occur in the perturbed areas. In the case of El Niño there is an increase in the surface and 500 mb temperatures as can be seen in figures 5 and 6, respectively. The largest variations of the temperatures occur in the regions where the sources of anomalies are strongest. As a consequence of the thermal wind balance the zonal wind is intensified as can be seen in figure 7. The highest deviations occur in the latitude belts inmediately situated northward (southward) from the perturbed areas in the NH (SH). Also the Hadley cell is intensified and the evaporation increases in the perturbed zones as is shown in figures 8 and 9, respectively. As a consequence there is an increase in the precipitation in the tropical region (fig. 10). An interesting aspect is that the variations are greater in the SH. This can be related to the fact that the greastest anomalie of SST is imposed in the latitude belt centered in 5°S as is indicated in Table 2 and also because the transports are also less in the SH.

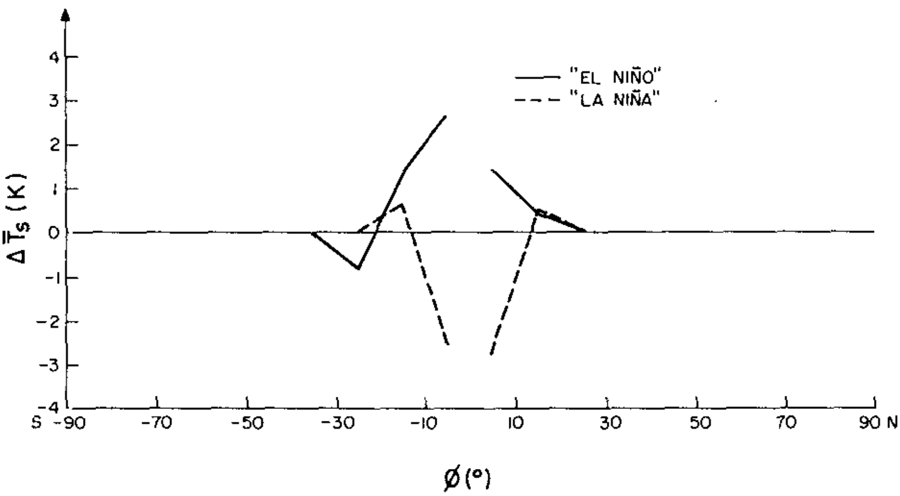

Figure 5.—Change (experiment with perturbation minus control) in the surface temperature for the El Niño (continuous line) and La Niña (broken line) experiments.

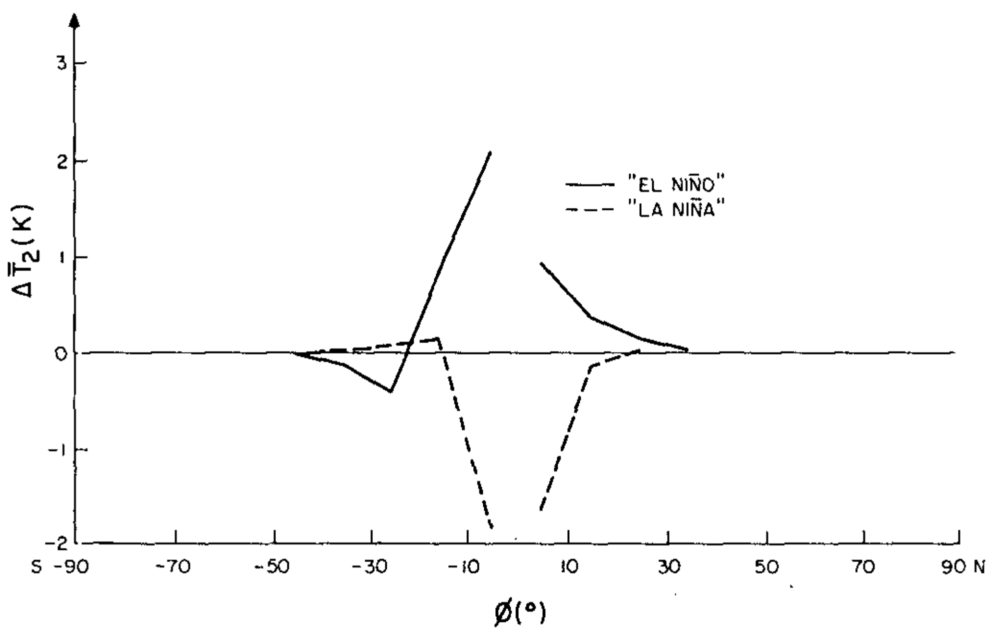

Figure 6.—Same as figure 5 but for the temperature at 500 mb level.

In the experiment of La Niña the deviations are opposite to those of the El Niño case: there is a decrease in the intensity of the zonal wind and in the surface and 500 mb temperatures; the Hadley cell is weak and the evaporation decreases so that the precipitation is reduced in the equatorial region.

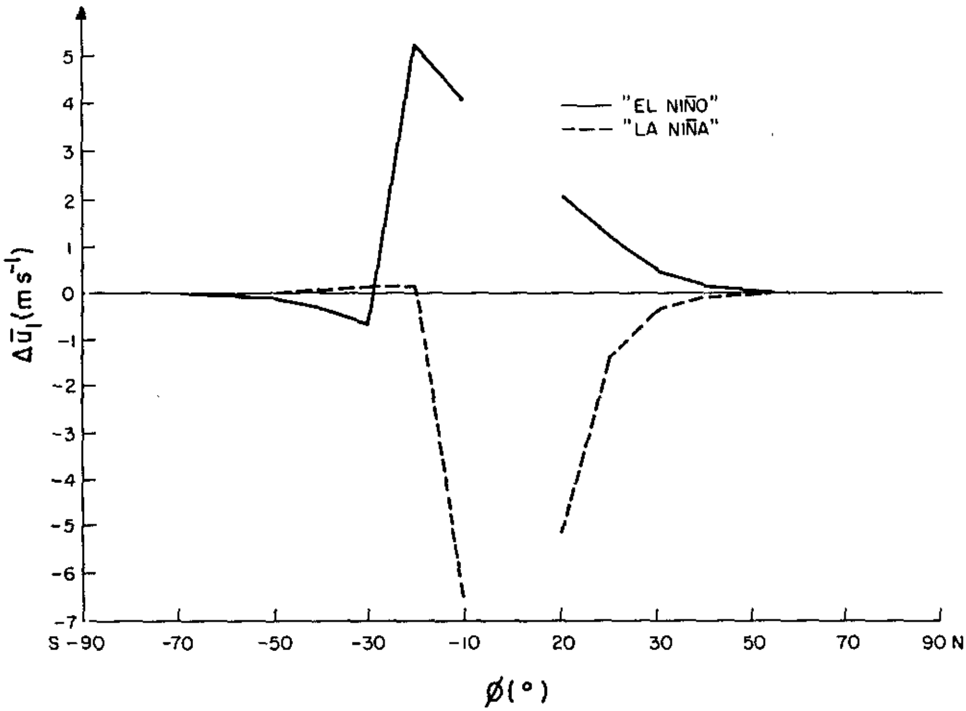

Figure 7.—Same as figure 5 but for the zonal wind at 250 mb level.

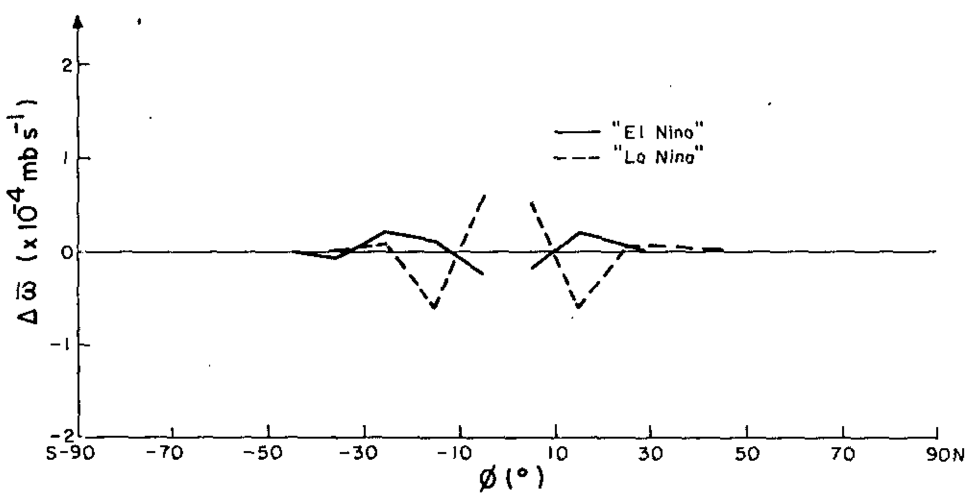

Figure 8.—Same as figure 5 but for $\bar{\omega}$.

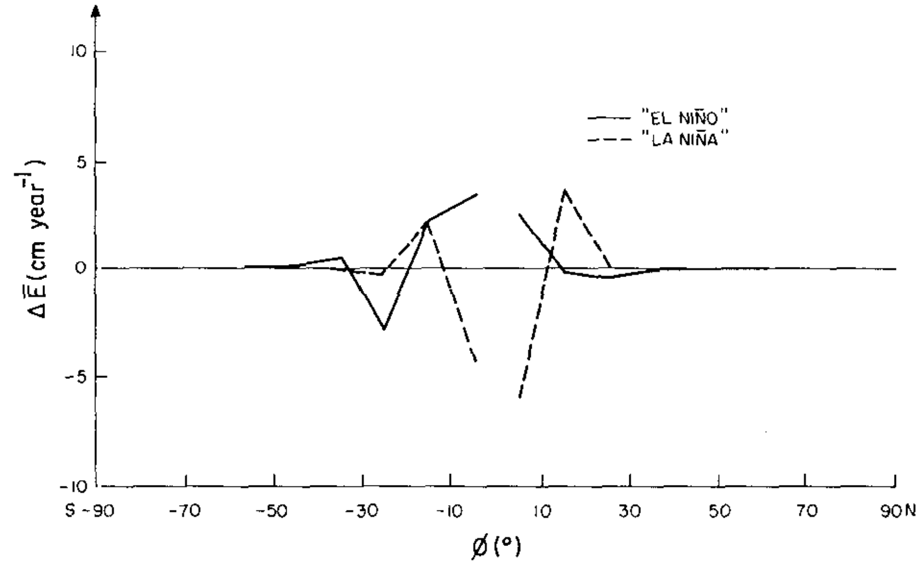

Figure 9.– Same as figure 5 but for evaporation.

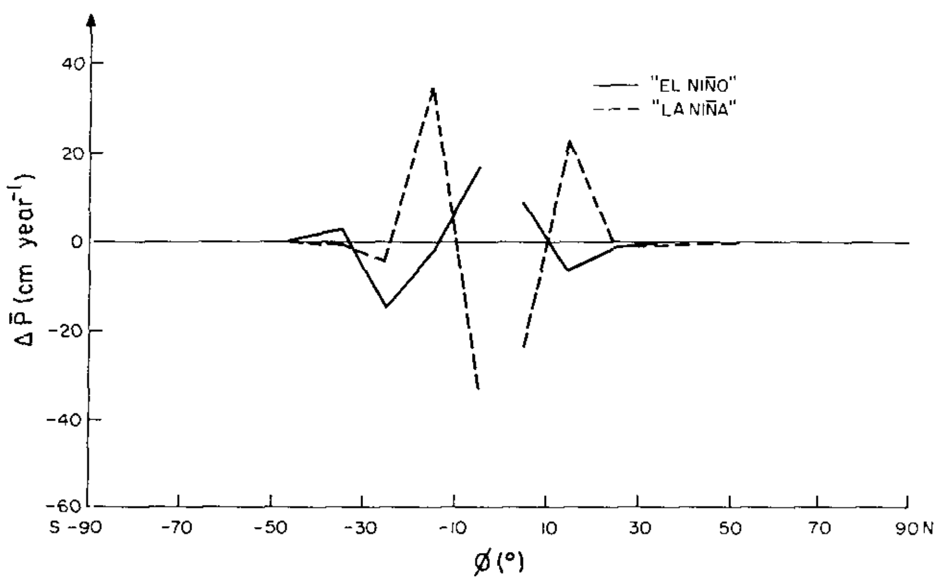

Figure 10. Same as figure 5 but for rainfall.

3. CLIMATE STUDIES WITH THE PRIMITIVE EQUATIONS MODEL

Although quasi-geostrophic models are adequate for the treatment of the dynamics of the atmosphere in the extratropical region, to simulate the mean meridional circulation boundary conditions in the tropical zone are necessary. When the interactions between the tropics and higher latitudes are considered the use of primitive equations is more appropriate. Moreover, a primitive equations model is better suited to conduct experiments on land surface alterations that occur in tropical and subtropical regions.

a) Description of the model

The climate model is a two-layer zonally averaged primitive equations in sigma-coordinate, similar to that used by Taylor (1980). The model includes parameterizations of friction, diabatic heating and large-scale eddies. However improvements have been made to permit the inclusion of some important climatic processes. Taylor's model is hemispheric (only the NH is considered) and has limitations, as regards the physical processes are considered. The present model is extended to the SH also, so that it is possible to study simultaneously the climatological features of both the hemispheres. Another advantage of the global model is the more realistic simulation of the Hadley cell because there is no boundary condition at the equator.

The zonally averaged primitive equations in the model are:

$$\frac{\partial}{\partial_t}(p^*\overline{u}) + \frac{1}{\mathrm{a}\cos\phi}\frac{\partial}{\partial\phi}(p^*\overline{u}\,\overline{v}\cos\phi) \pm 2p^*\dot{\overline{\sigma}}_2\overline{u}_2 - p^*f\overline{v} - p^*\overline{u}\,\overline{v}\ \frac{\tan\phi}{a} =$$

$$p^*\overline{F}_\lambda - \frac{1}{\mathrm{a}\cos\phi}\frac{\partial}{\partial\phi}(p^*\overline{u'v'}\cos\phi) \mp 2p^*\overline{\dot{\sigma}_2{}'u_2'} + p^*\overline{u'v'}\ \frac{\tan\phi}{a} \tag{16}$$

$$\frac{\partial}{\partial_t}p^*\overline{v}) + \frac{1}{\mathrm{a}\cos\phi}\frac{\partial}{\partial\phi}(p^*\overline{v}^2\cos\phi) \pm 2p^*\dot{\overline{\sigma}}_2\overline{v}_2 + p^*f\overline{u} + p^*\overline{u}^2\frac{\tan\phi}{a} =$$

$$-\frac{p^*}{a}\frac{\partial\Phi}{\partial\phi} - \frac{\cancel{\alpha p^*\overline{\alpha}}}{a}\frac{\partial p^*}{\partial\phi} + p^*\overline{F}_\phi - \frac{1}{\mathrm{a}\cos\phi}\frac{\partial}{\partial\phi} = (p^*\overline{v'^2}\cos\phi)\ \mp$$

$$\mp 2p^*\overline{\dot{\sigma}_2' v_2'} - p^*\overline{u'^2}\ \frac{\tan\phi}{a} \tag{17}$$

$$\frac{\partial}{\partial t}(p^*\overline{T}) + \frac{1}{\mathrm{a}\cos\phi}\frac{\partial}{\partial\phi}(p^*\overline{v}\,\overline{T}\cos\phi) \pm 2p^*\dot{\overline{\sigma}}_2\overline{T}_2 - \frac{p^*\overline{\alpha\omega}}{c_p} =$$

$$\frac{p^*}{c_p}\overline{H}_a - \frac{1}{a\cos\phi}\frac{\partial}{\partial\phi}(p^*\overline{v'T'}\cos\phi) \mp 2p^*\overline{\dot{\sigma}_2' T_2'} \tag{18}$$

$$p^*\bar{\dot{\sigma}}_2 = \frac{1}{4\ a\cos\phi}\frac{\partial}{\partial\phi}[p^*(\bar{v}_3 - \bar{v}_1)/2] \tag{19}$$

$$\Phi = \Phi_s + \frac{1}{2}p^*(\sigma_1\overline{\alpha}_1 + \sigma_3\overline{\alpha}_3) \pm \frac{1}{2}c_p\overline{\theta}_2 p_R^{-R/C_p}(\overline{p}_3{}^{R/C_p} - p_1{}^{R/C_p}) \tag{20}$$

$$\frac{\partial p^*}{\partial t} + \frac{1}{a\cos\phi}\frac{\partial}{}[p^*(\bar{v}_1 + \bar{v}_3)/2] = 0 \tag{21}$$

In these equations the deviation of the zonal average is indicated by a prime. The equations (16), (17) and (18) are applied at levels 1 (250 mb) and 3 (750 mb) so the subscripts 1 and 3 are omitted. When a equation is applied at a particular level the appropriate subscripts are attached. Further, the positive and negative sings in equations (16)-(21) refer to the two levels, the upper sign for level 1 and the lower sign for level 3.

Another improvement introduced in the present model in relation to Taylor's model is the incorporation of the physical processes not included in his model, namely the heat fluxes due to the release of latent heat, evaporation and subsurface conduction. The funtional form of the subsurface heat flux is taken from Saltzman (1986). The surface evaporation and the diabatic heating due to the release of latent heat are parameterized in a form similar to that given by Gutman *et al.* (1984). The other component of atmospheric and surface heating like the shortware and longwave radiation and small-scale convection have the functional forms similar to those proposed by Saltman (1986) adopted for a two-layer model by Taylor (1980). The functional forms of the diabatic heating are similar to those given in Table 1 with exception of surface evaporation flux which will be discussed latter in this section.

The model also includes the parameterization of the biofeedback mechanisms which link the surface state to the atmospheric processes, so that it is possible to study the interactions between the geobotanic state and climate. The method adopted is that given by Gutman *et al.* (1984). In Gutman *et al.* the geobotanic state, characterized by the land surface albedo and water availability parameter, is dependent on the radiative index of dryness defined as the ratio between the annual radiation balance and the annual precipitation. The parameterizations suggested by Gutman *et al.* consider only the NH. In the present model new parameterizations for the SH are included.

According to Gutman *et al.* method of parameterization the zonally averaged evapotranspiration is given by:

$$-\overline{H}_s(4) = (\overline{R}/L)(j_3\overline{w}a_2 + (1-j_3)\overline{w}_0 a_1),\ \overline{R} > 0 \qquad [22]$$

here $\overline{R}$ is the surface net radiation and a_1, a_2 and $\overline{w}_0$ are constants independent of the latitude. When $\overline{R} \leq 0$, the evapotranspiration is taken as zero.

The water availability parameter and the surface albedo have different parameterization for the NH (Gutman *et al.*, 1984) and SH (Franchito and Rao, 1990b):

Northern Hemisphere

$$\overline{w} = 1.23\ (\tanh \overline{D})/\overline{D} - 0.33, \quad \overline{D} > 0 \tag{23}$$

$$r_{s\ land} = \begin{cases} 0.07 + 0.06\ \overline{D} & , \quad \overline{D} \geq 1 \\ 0.2 - 0.002\ a_2\ \overline{R} & , \quad 0 < \overline{D} < 1 \\ \text{values from Sellers (1973)} & , \quad \overline{D} \leq 0 \end{cases} \tag{24}$$

Southern Hemisphere

$$\overline{w} = 0.6658 - 0.6989\ \overline{D} + 1.95\ \overline{D}^2 - 1.676\ \overline{D}^3 + 0.4208\ \overline{D}^4 \tag{25}$$

$$r_{s\ land} = \begin{cases} 0.06859 + 0.05622\ \overline{D} & , \quad \overline{D} \geq 1 \\ 0.22840 - 0.00138\ a_2\ \overline{R} & , \quad 0 < \overline{D} < 1 \\ \text{values from Sellers (1973)} & , \quad \overline{D} \leq 0 \end{cases} \tag{26}$$

where $\overline{D}$ is the radiative index of dryness given by:

$$\overline{D} = (\overline{R}/L\overline{P})\ a_2\ (j_3 + (1 - j_3)\ a_3) \tag{27}$$

where $\overline{P}$ is the zonally averaged precipitation and a_3 is a constant in NH. However, a_3 varies with the latitude in the SH and it is given by:

$$a_3 = 0.5 + 0.8\ \overline{D} \tag{28}$$

The model grid interval is 10° latitude and the initial state is an isothermal atmosphere (270 K) at rest. The equations are time integrated using an explicit scheme. The boundary conditions are:

$$\overline{\dot{\sigma}} = 0 \quad \text{at} \quad \sigma = 0,\ 1$$
$$\overline{v} = \overline{u} = 0 \ \text{at}\ \phi = 90°\ \text{N (S)}$$

b) Numerical experiments

The experiments carried out using the primitive equations model consider the climatic effects caused by land surface alterations, particulary the cases of deforestation and desertification. Deforestation and desertification are considered as the destruction of vegetation by overgrazing and excessive cultivation of land in tropical and semiarid regions, respectively. In each experiment a perturbation in the land surface albedo and in the water availability parameter (a diferent perturbation is specified in each case) is imposed in the latitude belts centered at 5° N (S) (deforestation case) and at 15° N 8 (S) (desertification case). The extention of each latitude belt is 10°.

In the case of deforestation the following changes have been made: the land surface albedo changes from 0.12 at 5° S and 0.1 at 5° N to 0.14 and $\overline{w}$ changes from 0.66 at 5° S to 0.61 and from 0.75 at 5° N to 0.52. This correponds to a change of tropical forest to savana.

In the case of desertification the land surface albedo changes from 0.13 at 15° S and 0.08 at 15° N to 0.17 and $\overline{w}$ changes from 0.65 at 15° S to 0.37 and from 0.64 at 15° N to 0.31. This corresponds to a change of grassland to desert.

The principal results (perturbed minus control) regarding the latitudinal variation of the surface net radiation, evapotranspiration, vertical velocity, precipitation and surface temperature are presented in figures 11-15, respectively. In these figures the results of the deforestation test are indicated by full line and the results of the desertification test by dashed line. The results of both the experiments are presented together because they are, in general, similar.

As can be seen in figure 11 there is a decrease in the surface net radiation in the perturbed areas in both the hemispheres. This is due to the increase of the land surface albedo and consequent reduction of the absorbed radiation flux.

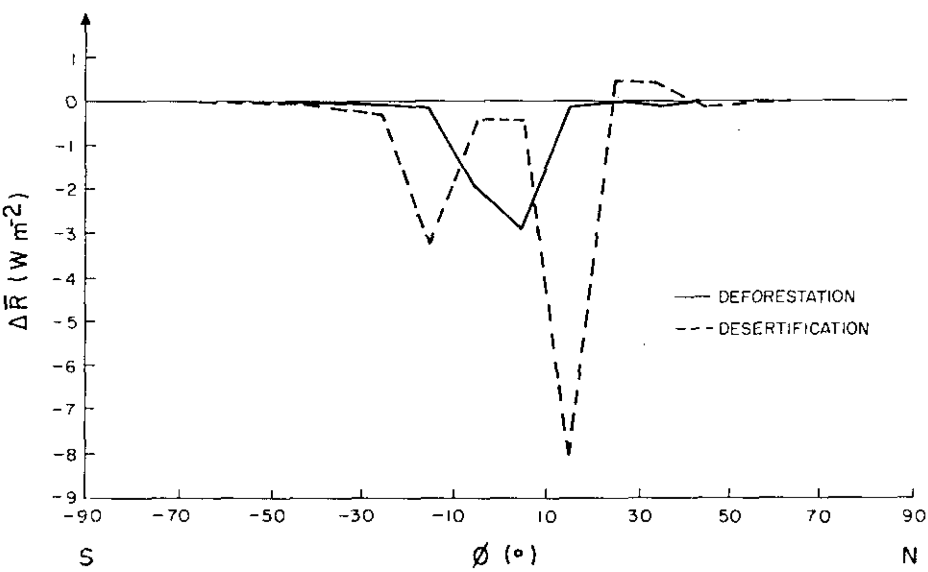

Figure 11. Change (experiment with perturbation minus control) in the net radiation for the deforestation (continuous line) and desertification (broken line) experiments.

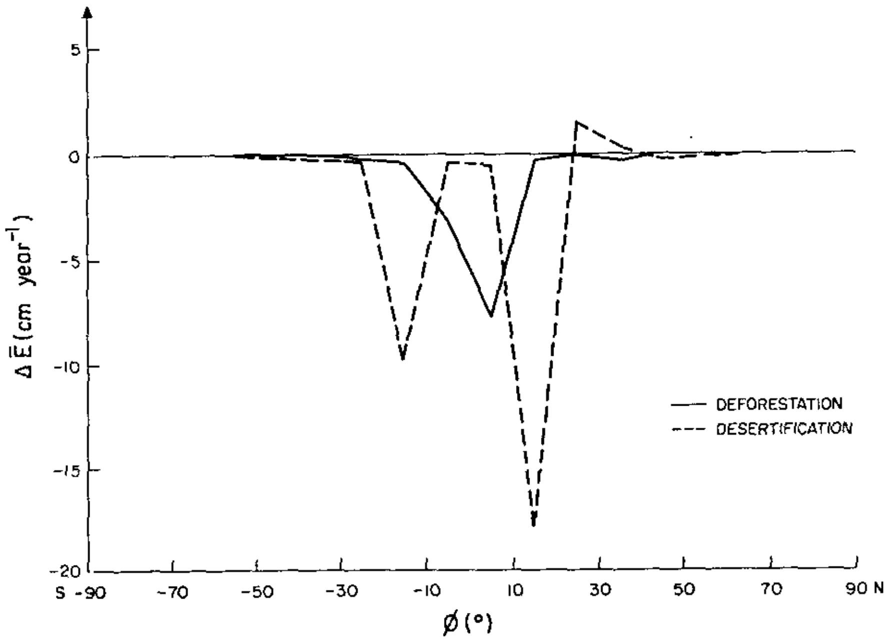

Figure 12.—Same as figure 11 but for evapotranspiration.

Figure 12 shows that there is a decrease in the evapotranspiration in the zones where the perturbations are imposed due to a decrease in the surface net radiation and in the water availability.

As can be noted in figure 13 the ascending branch of the Hadley cell is weaker in the deforestation case and the downward movement increases near 15°N (S). This can be interpretated as a weaking of the Hadley cell in the deforestation experiment. An intensification of the Hadley cell is obtained in the desertification experiment.

As a consequence of the increase of subsidence and the reduction of evapotranspiration in the perturbed regions there is a decrease in the precipitation in these areas as can be seen in figure 14.

Figure 15 shows that there is an increase of the surface temperature in the perturbed zones. This is due to the fact that the evapotranspiration decreases (because the decrease of the surface net radiation) in these regions. The effect of the decrease in the evaporative cooling overcomes that of the land surface albedo and consequently the surface temperature increases.

It can be seen also in figures 11-15 that the changes are greater in the perturbed areas in both the hemispheres. This agrees with Potter *et al.* (1979) and Gutman (1984). Another interesting aspect is that the changes are smaller in the SH. This can be justified by the smaller land fraction in this hemisphere.

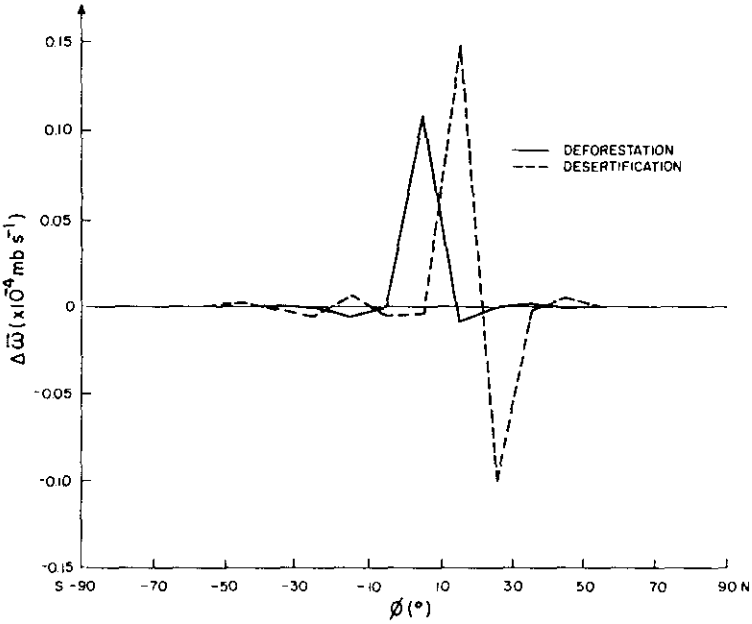

Figure 13. Same as figure 11 but for $\overline{\omega}$.

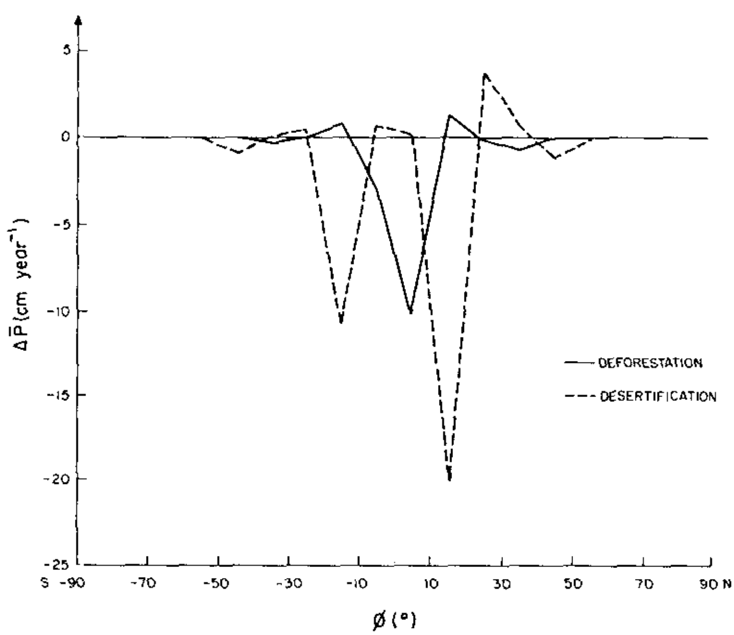

Figure 14. Same as figure 11 but for rainfall.

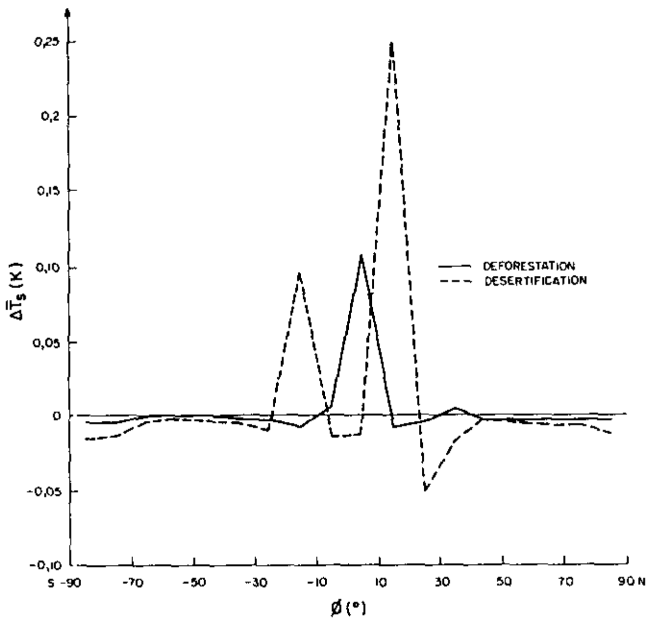

Figure 15.--Same as figure 11 but for surface temperature.

4. SUMMARY

Manifold physical processes which govern the climate system can be studied using a hierarchy of models. A brief review of the classification of climate models is given. The advantages of zonally averaged climate models (ZACM) are mentioned. Because of their intermediate posistion in the hierarchy of climate models, ZACM are useful both in the planing of more detailed general circulation models and generalizing much simpler one dimensional models. Furthermore ZACM have the advantage of consuming less computational time. Two ZACM are described, a simple quasigeostrophic (QG) model and a more complete primitive equations (PE) global model. Although QG model is adequate for the treatment of mid-latitude processes, a PE model is necessary for the study of the interaction between the tropics and higher latitudes.

One important quantity needed in the formulation of a QG model is the exchange coefficient for the QG potential vorticity. These exchange coefficients are determined by Franchito and Rao (1991) and the method for their determination is given.

The PE model developed is similar to the hemispheric model of Taylor (1980). However the model used here is a global model and includes additional physical processes not included by Taylor such as the evaporation cooling, rebase of latent heating of condensation and conduction of subsurface heating.

Annual mean conditions are simulated by both QG and PE models and these represent the control experiment. The experiments related to sea surface temperature anomalies consider El Niño and La Niña situations. The results show that in the case of El Niño the subtropical jet stream intensified, surface temperature, 500 mb temperature, evapotranspiration and precipitation increased in the perturbed region and the Hadley cell intensified. In the case of La Niña opposite situation occurred.

The PE model includes the parameterization of a biofeedback mechanism which links the surface state to the atmospheric processes. Thus, it is possible to study the interaction between the geobotanic state and the climate. For the NH parameterization of Gutman *et al.* (1984) are used and for the SH new parameterizations are derived.

Two experiments are conducted regarding the effect of surface state alterations on climate: 1) deforestation and 2) desertification. The results show that the change in the evapotranspiration rather than the change in the surface albedo is the predominant effect in regulating the change in the surface temperature.

Acknowledgements

Thanks are due to Dr. P. Satyamurty for carefully going through the manuscript.

REFERENCES

Adem, J. (1962): On the theory of the general circulation of the atmosphere. *Tellus*, **14**, 102-115.

Budyko, M. Y. (1969): The effect of solar radiation variations on the climate of the earth. *Tellus*, **21**, 611-619.

Charney, J. G., P. H. Stone and W. J. Quirk (1975): Drought in the Sahara: a biogeophysical feedback mechanism. *Science*, **187**, 434-435.

– –, and M. Stern (1962): On the stability of internal baroclinic jets in a rotating atmosphere. *J. Atmos. Sci.*, **19**, 159-172.

Dickinson, R. E. (1989): Modeling the effects of Amazonian deforestation on regional surface climate: a review. *Agric. For. Meteor.* **47**, 339-347.

—, A. Henderson-Sellers, P. J. Kennedy and M. F. Wilson (1986): Biosphere-atmosphere transfer scheme (BATS) for the NCAR Community Climate Model. *NCAR Tech.* Note 275.

, and A. Henderson-Sellers (1988): Modeling tropical deforestation: a study of GCM land-surface parameterizations. *Quart. J. Roy. Meteor. Soc.* **114**, 439-462.

Edmon, H. J., B. J. Hoskins and M. C. McIntyre (1980): Eliassen-Palm cross sections for the troposphere. *J. Atmos. Sci.* **37**, 2600-2616.

Ellsaesser, H. W., M. C. McCracken, G. L. Potter and F. M. Luther (1976): An additional model test of positive feedback from high desert albedo. *Quart. J. Roy. Meteor. Soc.* **102**, 655-666.

Franchito, S. H. and V. B. Rao (1991): *Quasi-geostrophic potential vorticity transport in the Northern and Southern Hemispheres and simple climate models. J. Meteor. Soc. Japan,* **69**, 233-239.

——, and —— (1990): Climatic change due to land surface alterations. (Submitted to *Clim. Change).*

Green, J. S. A. (1970): Transfer properties of large-scale eddies and the general circulation of the atmosphere. *Quart. J. Roy. Meteor. Soc.* **96**, 157-185.

Gutman, G. (1984): Numerical experiments on land surface alterations with a zonal model allowing for interaction between the geobotanic state and climate. *J. Atmos. Sci.* **41**, 2679-2685.

——, G. Ohring and J. H. Joseph, (1984): Interaction between the geobotanic state and climate: a suggested approach and a test with a zonal model. *J. Atmos. Sci.* **41**, 2663-2678.

Harvey, L. D. D. (1988a): A semianalytic energy balance climate model with explicit sea ice and snow physics. *J. Climate,* **1**, 1065-1085.

—— (1988b): On the role of high altitude ice, snow and vegetation feedbacks in the climatic response to external forcing changes. *Clim. Change,* **13**, 191-226.

Idso, S. B. and J. F. B. Mitchell (1989): The search for CO_2/trace gas greenhouse warming. *Theor. Appl. Climatol.* **40**, 101-102.

Jones, P. D., S. C. B. Raper and T. M. L. Wigley (1986a): Northern Hemisphere air temperature variations: 1851-1984. *J. Climate Appl. Meteor.* **25**, 161-179.

——, ——, and —— (1986b): Southern Hemisphere air temperature variations: 1851-1984. *J. Climate Appl. Meteor.* **25**, 1213-1230.

Jung. H. J., and W. Bach (1987): The effects of aerosols on the response of a two-dimensional zonally-averaged climate model. *Theor. Appl. Climatol.* **38**, 222-233.

Karoly, D. J. (1987): Southern Hemisphere temperature trends: a possible greenhouse gas effect?. *Geophys. Res. Lett.* **14**, 1139-1141.

Lau, N. C. and A. H. Oort (1985): Response of a GFDL general circulation model to SST fluctuations observed over the tropical Pacific during the period 1962-1976. Proc. 16th Int. Liege Colloq. on Ocean Hydrodynamics.

Lindzen, R. S. (1990): Some coolness concerning global warming. *Bull. Amer. Meteor. Soc.* **71**, 288-299.

Manabe, S. and R. T. Wetherald (1967): Thermal equilibrium of the atmosphere with a given distribution of relative humidity. *J. Atmos. Sci.* **24**, 241-259.

Mintz, Y., P. J. Sellers and C. J. Willmott (1983): On the desing of a interactive biosphere for the GLASS general circulation model. NASA Tech. Memo. 84973, Goddard Space Flight Center, 57 pp.

Moura, A. D. and J. Shukla (1981): On the dynamics of drought in northeast Brazil: Observations, theory and numerical experiments with a general circulation model. *J. Atmos. Sci.* **38**, 2653-2675.

Ohring, G. and S. Adler (1978): Some experiments with a zonally averaged climate model. *J. Atmos. Sci.* **35**, 186-205.

Oort, A. H. and E. M. Rasmusson (1971): Atmospheric circulation statistics. NOAA Prof. Pap. No 5, U. S. Dept. of Commerce, Rockville, MD, 323 pp.

Potter, G. L., H. W. Ellsaesser, M. C. MacCracken and F. M. Luther (1975): Possible climatic impact of tropical deforestation. *Nature,* **258**, 697-698.

——, ——, ——, and ——, (1979): Climate experiments: albedo experiments with a zonal atmospheric model. *GARP Publ. Ser.* No 22, WMO, 995-1001.

——, and R. D. Cess (1984): Background trotospheric aerosols: incorporation within a statistical-dynamical climate model. *J. Geophys. Res.* **89**, 9521-9526.

Randel, W. J. and J. L. Stanford (1985): The observed life cycle of a baroclinic instability. *J. Atmos. Sci.* **42**, 1364-1373.

Rasool, S. I. and S. H. Schneider (1971): Atmospheric carbon dioxide and aerosols: effects of large increases on global climate. *Science,* **173**, 138-141.

Richtmeyer, R. D. (1957): Difference methods for initial-value problems. 1st ed. Interscience (see p. 101).
Saltzman, B. (1968): Steady-state solutions for the axially-symmetric climate variables. *Pure Appl. Geophys.* **69**, 237-259.
—— (1978): A survey of statistical-dynamical models of terrestrial climate. *Advances in Geophysics*, Vol. 20, Academic Press, 183-304.
—— and A. D. Vernekar (1968): A parameterization of the large-scale eddy flux of relative angular momentum. *Mon. Wea. Rev.* **96**, 854-857.
——, and —— (1971): An equilibrium solution for the axially-symmetric component of the earth's macroclimate. *J. Geophys. Res.* **76**, 1498-1524.
——, and —— (1972): Global equilibrium solutions for the zonally-averaged macroclimate. *J. Geophys. Res.* **77**, 3936-3945.
Schneider, S. H. and R. E. Dickinson (1974): Climate modeling. *Rev. Geophys. Space Phys.*, **12**, 447-493.
Sela, J. and A. Wiin-Nielsen (1971): Simulation of the atmospheric annual energy cicle. *Mon. Wea. Rev.* **99**, 460-468.
Sellers, P. J., Y. Mintz, Y. C. Sud and A. Dalcher (1986): A simple biosphere (SiB) model for use within general circulation models. *J. Atmos. Sci.* **43**, 505-531.
Sellers, W. D. (1969): A global climatic model based on the energy balance of the earth-atmosphere system. *J. Appl. Meteor.* **8**, 392-400.
Shukla, J. and J. M. Wallace (1983): Numerical simulation of the atmospheric response to equatorial Pacific sea surface temperature anomalies. *J. Atmos. Sci.* **40**, 1613-1630.
——, C. A. Nobre and P. Sellers (1990): Amazonia deforestation and climatic change. *Science*, **247**, 1322-1325.
Stone, P. H. (1974): The meridional variation of the eddy heat fluxes by baroclinic waves and their parameterizations. *J. Atmos. Sci.* **31**, 444-456.
——, and M. S. Yao (1987): Development of a two-dimensional zonally averaged statistical-dynamical model. Part II: the role of eddy momentum fluxes in the general circulation and their parameterization. *J. Atmos. Sci.* **44**, 3796-3786.
Taylor, K. E. (1980): The role of mean meridional motions and large-scale eddies in zonally averaged circulations. *J. Atmos. Sci.* **37**, 1-19.
Wiin-Nielsen, A. (1986): On simple estimates of the impact of heating anomalies in the zonal atmospheric circulation. *Annal. Geophy.* **4**, 365-376.
——, and J. Sela (1971): On the transport of quasi-geostropic potential vorticity. *Mon. Wea. Rev.* **99**, 447-459.